ELSEVIER

Journal of Power Sources 108 (2002) 106–112

JOURNAL OF POWER SOURCES

www.elsevier.com/locate/jpowsour

Flow network analysis application in fuel cells

Z. Ma*, S.M. Jeter, S.I. Abdel-Khalik

G.W. Woodruff School of Mechanical Engineering, Georgia Institute of Technology, Atlanta, GA 30332-0405, USA

Received 15 October 2001; accepted 17 December 2001

Abstract

This paper deals with network flow analysis and its application to the calculation of flow distribution within fuel cells. The generated node and loop equations for the network analysis are presented. In order to accommodate changes in cell design, i.e. changes in flow network topology, the analysis includes automatic loop equation generation based on topology analysis and network search algorithm. The calculated flow distributions were in excellent agreement with experimental data.

Keywords: Fuel cells; Flow distribution; Molten carbonate fuel cell

1. Introduction

Flow networks exist in a wide range of practical systems, including transportation systems, water distribution systems, thermal systems, as well as information flow through the Internet. In a thermal system, flow network analysis serves a critical design purpose involving fluid flow, heat and mass transfer for equipments such as heat exchanger, boiler and most recently, fuel cell stacks. Analysis of the flow distribution provides a better understanding of the performance of such network flow systems.

In a fuel cell generating system, fuel cells are connected electrically in series to create a fuel cell stack. Usually, fuel or oxidant flows through the fuel cell in multiple channels arranged in a complex flow network. The flow distribution within a fuel cell stack is a major concern facing fuel cell designers since it has a significant impact on fuel cell performance and efficiency [1]. Numerous studies dealing with the electrochemical and material aspects of fuel cells have been performed. However, to reduce manufacturing costs and improve performance, better understanding of the fuel and oxidant species transport processes within the fuel cell stack is critical and is still an open question. Hirata and Hori [2] have studied the effects of the gas flow uniformity on cell performance. They found that a uniform inlet flow distribution results in improved performance for the co-flow fuel cell configuration. To achieve uniform flow, many designs often use a complex flow network, and inevitably, increase the stack cost, (Sadowski et al. [3]).

Analysis of the fuel cell stack performance requires knowledge of the flow distribution within the stack. For this purpose, computational fluid mechanics (CFD) presents a helpful tool. This method is limited to simple geometric configurations with few flow channels. However, flow through the distribution manifold of a fuel cell generally forms a complex flow network (Fig. 1), which makes CFD computations exceedingly costly and time consuming due to the difficulty of generating complex computational grid. Hence, flow network analysis offers a useful tool for such applications. Various mathematical techniques and computer software have been developed for solving the problem of flow and pressure distributions in network systems [5]. However, these methods have restrictions and cannot currently be used to estimate the fuel cell stack performance. With its long tested history in solving network flow analysis problems for thermal systems, SINDA/FLUINT [6] has a great potential in dealing with the flow distribution issue within fuel cell stack designs. SINDA/FLUINT may also be extended to calculate the parameter profiles within a fuel cell stack, as long as an adequate fuel cell model can be implemented into its network analysis procedure.

In this investigation, methods for complex network flow analysis have been developed and compared with experiments. The presentation will begin with simple distribution systems with manually generated node and loop equations. In order to accommodate design changes, i.e. changes in the flow network topology, an automatic scheme for loop equation generation based on topology analysis and network search algorithm will then be presented.

* Corresponding author. Present address: Fuelcell Energy Inc., 3 Great Pasture RD, CT Danbury 06813, USA. Tel.: +1-203-205-2487; fax: +1-203-825-6100.
E-mail address: zma@fce.com (Z. Ma).

0378-7753/02/$ – see front matter
PII: S0378-7753(02)00008-3

Nomenclature

A_s	cross-section area (m^2)
A_w	wall area of a channel (m^2)
b	the number of branches
C_f	frictional coefficient
d	the number of nodes
D_H	hydraulic diameter (m)
E	energy term
G	mass flux (kg/m^2s)
H_{ser}	the energy losses through the loop
H_L	the head loss in the branch
K	the loss coefficient
l	the number of loops
$\dot{m}$	mass flow rate (kg/s)
Por p	pressure (Pa)
Re	Reynolds number
S	sign function of flow direction with respect to node (+1, −1 or 0)
u	velocity in x direction (m/s)
$\overline{u}$	average flow velocity in a channel (m/s)
x	x coordinate direction
Subscripts	
i	branch number
j	node or loop number
Greek symbols	
δ	gas channel height (m)
μ	dynamic viscosity of solution ($N\,s/m^2$)
θ	sign function for branch flow direction (+1, −1 or 0)
ρ	mass density (kg/m^3)
τ	shear stress (N/m^2)
ξ	pressure loss coefficient

2. Network analysis

A complex flow system can be reduced into a graphical and numerical construction as illustrated in Fig. 2. In this graph, nodes and branches are defined and numbered. From the graph structure, a simple loop starting from one node, passing through some closed branches, and returning to the original node, is identified. The network flow distribution into the various branches can be computed based on application of the conservation principles at the nodes and through the flow loops.

Consider a flow network as shown in Fig. 1. The fundamental equation to be satisfied is mass conservation for a node, which states that the flow into and out of each node should be equal,

$$\sum_{\text{inlet}} \dot{m}_i = \sum_{\text{outlet}} \dot{m}_i \tag{1}$$

or

$$\sum_{i=1}^{d+l} S_{ji}\dot{m}_i = 0 \quad (j = 1, 2, \cdots, d) \tag{2}$$

where S_{ji} represents the sign of flow in branch i relative to node j, and the subscript i represents the branch number. S_{ji} is equal to +1 when fluid flows into the node, and is equal to −1 when fluid flows out from the node. S_{ji} is 0 if branch i has no connection with node j. Here d is the total number of nodes, while l is the total number of loops.

For each of the loops in the network (Fig. 1), i.e. $j = d + 1$, $d + 2$, …, $d + l$, the energy conservation equation can be written as

$$H_{ser} - \sum E_p = \Delta E \tag{3}$$

where H_{ser} is the energy losses through the loop, E_p is the energy input to the fluids by pump or compressor, and ΔE is the difference in pressure head in source nodes.

The head loss in each series channel add to the energy loss, H_{ser}, that is,

$$H_{ser} = \sum H_{L,ij} \tag{4}$$

where $H_{L,ij}$ represents the head loss of loop j resulting from friction associated with flow through branch i. It can be expressed in a general form as

$$H_{L,ijr} = \sum K_i (\dot{m}_i)^{n_i} \tag{5}$$

where K_i is the loss coefficient for different head losses and the exponent n_i can vary among the components.

For the interior flow distribution within a fuel cell stack (see for example Fig. 1), no energy input and head change through the node is present. Hence, the energy input term, E_p, and the pressure difference in source nodes, ΔE, can be neglected. Therefore, from Eq. (3), the loop or energy equations state that the sum of pressure changes around any loop j should be zero, i.e.

$$\sum_{i=1}^{d+l} \theta_{ji}\,\Delta P_i = 0 \quad (j = d + 1, d + 2, \ldots, d + l) \tag{6}$$

where θ_{ji} is a sign convention representing the direction of flow in branch i relative to loop j. θ_{ji} is +1 when fluid flows in the same direction as marked in the figure and −1 if the fluid flow direction is opposite to the marked direction. θ_{ji} is 0 if branch i does not belong to loop j.

The pressure drop of branch i in flow loop j is composed of friction loss and local loss, which can be written in the form of

$$\Delta P_i = \Delta P_{\text{inlet}} + \Delta P_{\text{outlet}} + \Delta P_{\text{bend}} + \tau \frac{A_w}{A_s} \tag{7}$$

where τ is the shear stress, which can be found from

$$\tau \frac{A_w}{A_s} = C_f \frac{\rho}{2} \overline{u}_i^2 \frac{A_w}{A_s} = C_f \frac{\overline{u}_i}{2} \frac{A_w}{A_s^2} \dot{m}_i \tag{8}$$

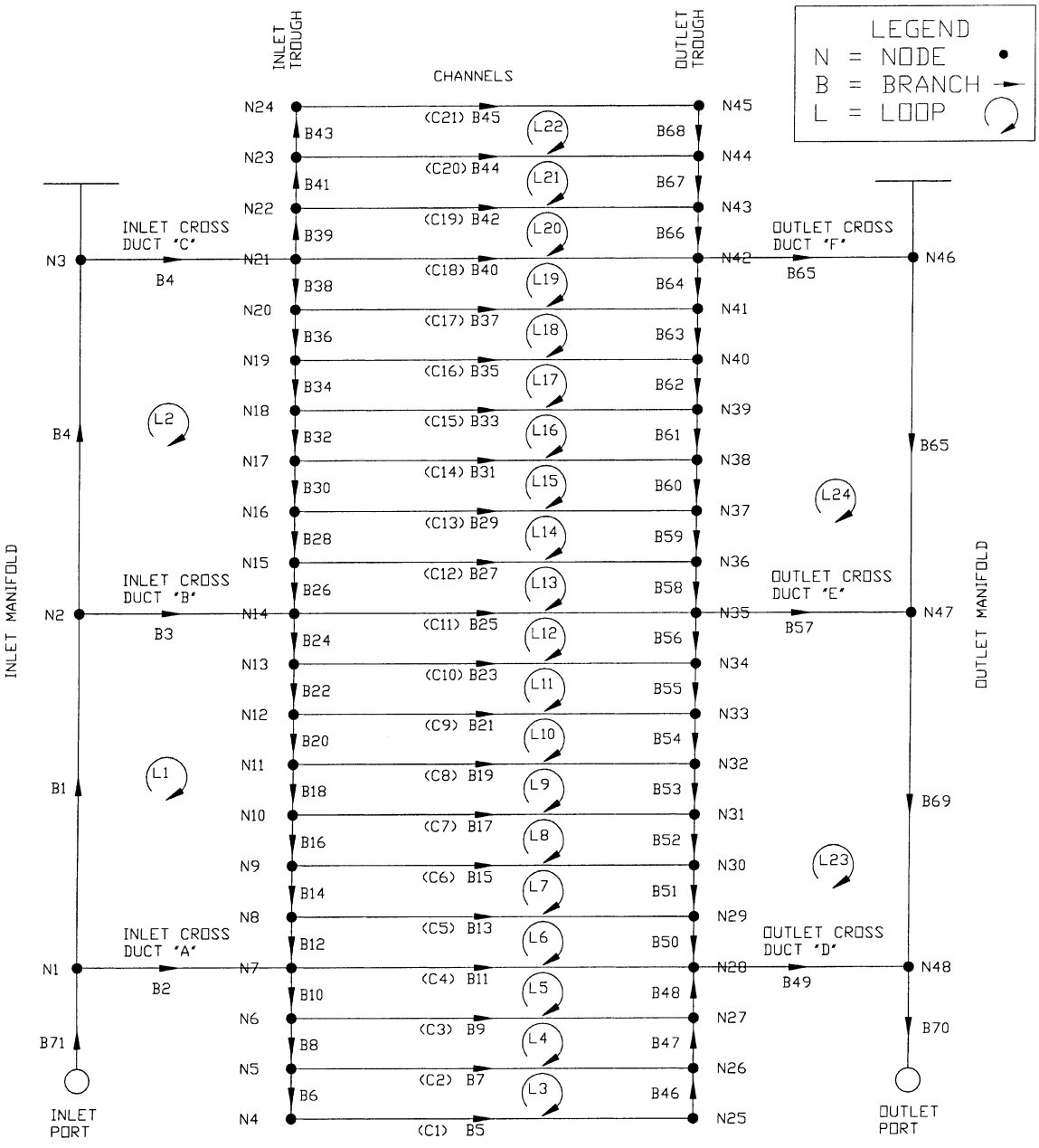

Fig. 1. Sample diagram for a complex flow network.

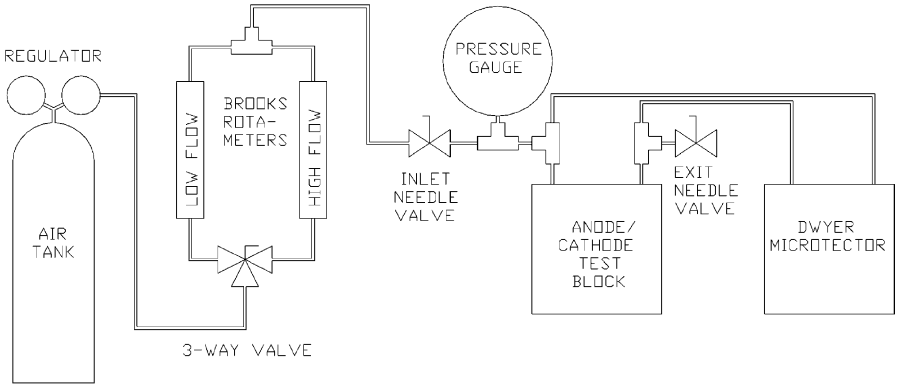

Fig. 2. Schematic drawing of pressure drop experiment set-up.

C_f is the friction coefficient, which is dependent on the Reynolds number and the path cross-sectional geometry shape. Here, we use the real cross-sectional area A_s and wall area A_w to account for the flow velocity and shear force. Using the appropriate friction coefficient, the model can be tailored to any flow path shape and thus overcomes the shortcomings of commercial network analysis codes.

The transitional loss can be estimated in terms of the loss coefficients

$$\Delta P_{\text{inlet}} = \xi_{\text{inlet}} \frac{\rho}{2} \overline{u}_i^2 = \xi_{\text{inlet}} \frac{\overline{u}_i}{2A_s} \dot{m}_i \tag{9}$$

$$\Delta P_{\text{bend}} = \xi_{\text{bend}} \frac{\rho}{2} \overline{u}_i^2 = \xi_{\text{bend}} \frac{\overline{u}_i}{2A_s} \dot{m}_i \tag{10}$$

$$\Delta P_{\text{outlet}} = \xi_{\text{outlet}} \frac{\rho}{2} \overline{u}_i^2 = \xi_{\text{outlet}} \frac{\overline{u}_i}{2A_s} \dot{m}_i \tag{11}$$

where the subscripts inlet, outlet and bend represent inlet, outlet and bend, respectively. The loss coefficients $\xi_{\text{inlet}}, \xi_{\text{outlet}}$, and ξ_{bend} for various types of junctions are listed in Idelchik's handbook [4]. The transitional loss coefficient in reference [4] is expressed as a function of the connection geometry, along with the ratio of the flow rates among branches. It, therefore, accurately includes the factors affecting the local pressure loss, which is frequently assumed to be constant. Substituting Eqs. (9)–(11), we can express the pressure drop across branch i in the following form

$$\begin{aligned} \Delta P_i &= \Delta P_{\text{inlet}} + \Delta P_{\text{outlet}} + \Delta P_{\text{bend}} + \tau \frac{A_w}{A_s} \\ &= \left(\xi_{\text{inlet}} \frac{\overline{u}_i}{2A_s} + \xi_{\text{outlet}} \frac{\overline{u}_i}{2A_s} + \xi_{\text{bend}} \frac{\overline{u}_i}{2A_s} + C_f \frac{\overline{u}_i}{2} \frac{A_w}{A_s^2} \right) \dot{m}_i \\ &= K_i \dot{m}_i \end{aligned} \tag{12}$$

The preceding equations can be written in a globally linearized form with K_i being the globally linearized flow coefficients. The globally linearized loop equations, along with the inherently linear node equations, form a set of b linearized equations, where b is the branch number $(d + l)$. In matrix form, this can be represented by:

$$\begin{pmatrix} S_{ji} \\ \theta_{ji} K_i \end{pmatrix} \dot{m}_i = B \quad (j = 1, 2, \ldots, b) \tag{13}$$

The mass flow conservation equations are linear, but the constitutive equations for the pressure drops are only linear for low Reynolds number (laminar flow) without transitional losses. In such cases, Eq. (13) can be readily solved by the matrix method. For cases involving transitional losses and/or turbulent flow, a system of non-linear equations results, which can be solved by a multi-variable Newton's method.

The global linearization method used to solve Eq. (13) is based on an iterative procedure. The computation starts from a set of guessed flow rates, which determines the coefficient, K_i, of Eq. (12), and solve a new set of flow rates by any solver for the system of linear equations. An iterative procedure is performed for generating a new solution until the difference between the new solution and the previous solution converge within a specified tolerance. The global linearization method relaxes the solution process compared to a solver for non-linear system of equations. The network analysis program based on the above numerical scheme has been assigned the name of "GT code."

Following the procedure described above, the network equations could be generated manually. However, this would limit the model's flexibility, that is, if the flow network were to be modified during the system design process, one needs to redo the entire process manually. To overcome this drawback, the evolution program method developed by Savic and Walters [7], was adopted. The hydraulic solver uses a method based on loop equations, namely, the linear theory method. Network topology analysis is performed using depth-first-search and breadth-first-search algorithms that are devised to ensure the connectedness of a network and to enable easy identification of loops. The model to be developed will enable rapid evaluation of a network for different topological conditions (i.e. the connectivity of the nodes caused by different piping configurations).

The automatic network analysis code written in Fortran90 using the search algorithm [7] has been tested. The automatically generated loop equations were successfully solved by using the global linearization method. The results from both the manually generated network equation and the automatic network analysis are compared with experimental data, as well as the result from SINDA/FLUINT.

3. Experimental verification of flow network analysis

The network analysis model is based on both the hydraulic energy principles and the automatic search method. The schematics used in the network flow code are presented in Fig. 1. Channels provide a passage for supplying gases to the fuel cells. A model of the fuel cell flow network was set-up. A multi-manifold flow scheme was used to ensure uniform flow through the different gas channels. Gas stream flows into the manifold and three cross-ducts distribute the flow stream into the trough. Two manifolds were located at each end of the channels and connected by the cross-ducts.

In Fig. 1, each node and each branch are numbered sequentially. The flow directions are assumed and marked by the arrows. If the flow direction inside a channel is consistent with the direction assumed, then the computed flow rate will be positive. Otherwise, the sign of the computed flow rate will be negative. For a manually generated loop equation, the loop can be easily identified as shown in the figure. It is intuitive to choose the minimum loop, which includes the smallest number of branches and the independent condition for the loop equation will be automatically satisfied.

3.1. Measurements to verify the network analysis scheme

Experiments were run to measure the total pressure drop in the 21 channel flow network of Fig. 1 in order to check the adequacy of the various empirical loss coefficient data used in the network analysis model. An experimental apparatus was designed, built and instrumented for that purpose (Fig. 2).

Referring to Fig. 2, air is supplied by a compressed air cylinder fitted with an adjustable pressure regulator and pressure gauge. The volumetric flow rate is measured using a pair of rotameters (Brooks Instruments), one for low flow rates, and the second for high flow rates. A three-way valve allows the user to easily switch between the two rotameters. Air pressure at the inlet to the test block is regulated using a test pressure gauge. Flow rate and back pressure are controlled by a pair of needle valves, one at the inlet to the test block, and the other at the exit. The pressure drop across the test block is measured using a Dwyer Microtector, capable of detecting a pressure change down to 0.0002 in. of water (0.05 Pa).

Experiments were run at regulated pressures of 193.1 kPa to measure the total pressure drop in the flow network system. In the flow network analysis computation using both the GT code and SINDA/FLUINT, the total pressure drop from the network inlet to its outlet was also calculated. Comparisons between measurements and calculations are shown in Fig. 2.

In the laminar fully developed flow regime, the friction coefficient is inversely proportional to the Reynolds number. Therefore, the friction loss along the flow path varies linearly with the increase in the fluid flow rate. However, the transitional loss through a junction is expressed as $C_f \rho u^2/2$, where a loss coefficient is defined as C_f. The pressure drop through a junction increases with the flow rate in a square power form. Hence the total pressure drop through the flow network varies with the flow rate in a quadratic form.

The SINDA/FLUINT analysis does not include the empirical relations for the transitional losses corresponding to each flow junction conditions. Instead, the recommended constant value for a conjunction was used. Therefore, the predicted SINDA/FLUINT pressure drop curve appears lower and more linear than the GT code prediction. The experiments show a strong non-linear effect due to the quadratic variation of transitional losses. The simulated results presented in Fig. 3 show an acceptable agreement with experimental data; the calculated error, with reference to the total pressure difference along the manifold, is about 4%.

Another experiment was performed to ascertain if laser Doppler velocimetry (LDV) could be used to measure detailed flow velocity distributions in the various channels. LDV measurements are based on the principle that two intersecting laser beams produce a fringe pattern within a very small target area. Pulses of light reflected off particles passing through the fringe pattern are detected by a photomultiplier. Signals from the photomultiplier are sent to a signal processing system, which converts the pulse rate to a velocity value. Given a sample size of several thousand particles passing through the target area, a velocity distribution can be produced and the average velocity of a fluid may be determined.

Experimental error in the LDV measurements is largely due to the many factors that can affect the measurements. Most important among these factors is the placement of the target beam. Other factors include small fluctuations in the flow rate, electrical noise, reflectivity of the surface of the channel, density of the seeding particles, and the presence of tiny bubbles in the channel. It is concluded that while the LDV measurements are useful for identifying trends, extra-

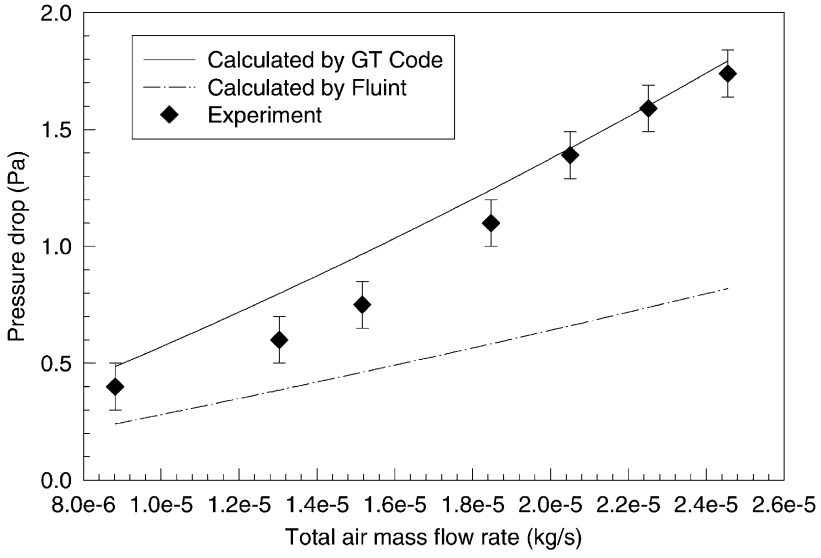

Fig. 3. Measured vs. predicted pressure drop across cathode at an inlet pressure of 193.1 kPa.

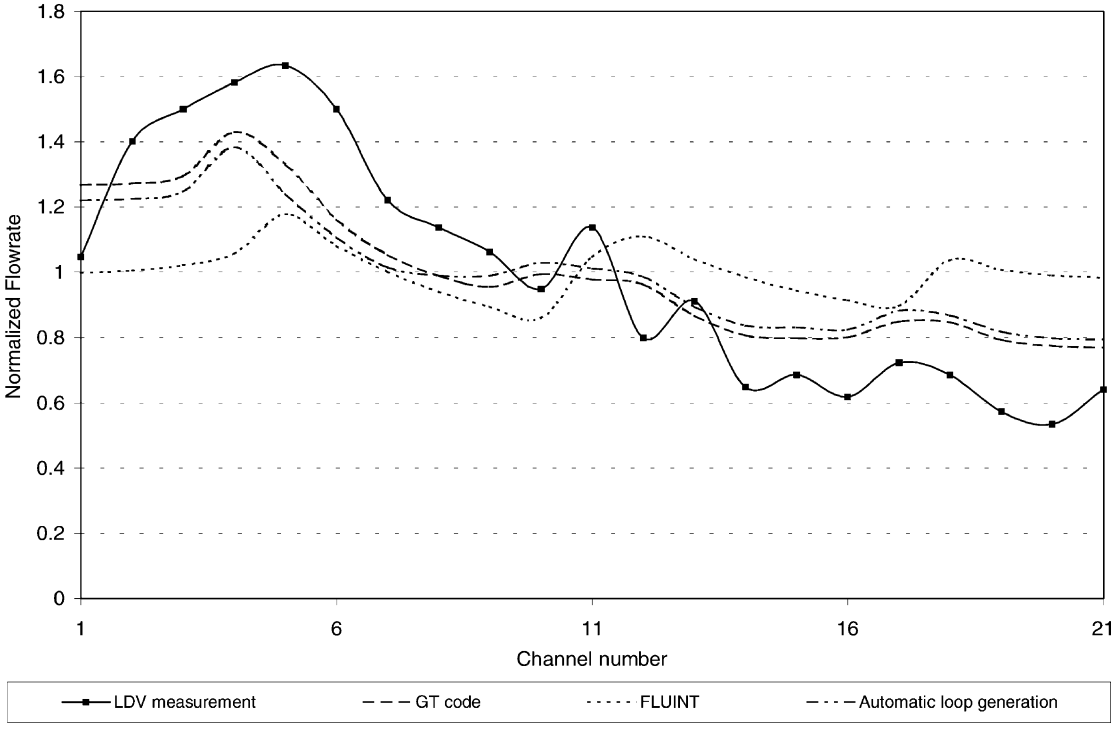

Fig. 4. Flow distributions through channels by LDV measurements, along with calculations from SINDA/FLUINT, GT network analysis code, and the automatic flow network generation analysis code.

ordinary measures are needed to assure accuracy of the velocity measurements for the geometries and flow conditions of interest in this study. The care and attention to detail taken in this study resulted in velocity distributions consistent with prediction of the codes previously validated by the pressure drop measurements.

In Fig. 1 the channel number C1 denotes the bottom channel, and the channel number C21 indicates the top channel of the schematic flow network. Fig. 4 displays the flow distributions through the 21 channel in the flow network shown in Fig. 1 comparing LDV measurements, the predicted normalized flow rate from SINDA/FLUINT, GT network analysis code, and automatic network equation generation code.

In the LDV experiment, the pressures at the inlet manifold and at the outlet remain constant for a certain flow rate. As exhibited in Fig. 4, the LDV experimental data show a certain scatter due to the instabilities of the decelerated flow. The simulated results present an acceptable agreement with experimental data; the error, which is calculated with reference to the channel with the highest deviation, is about 4.7%. Thus, it can be concluded that the flow in the inlet manifold is sufficiently well simulated by the GT code. The result by automatic network equation generation agrees well with the GT code as well as the LDV experimental data. The SINDA/FLUINT result follows the flow distribution trend well compared with the LDV measurement, but the predicted distribution is more uniform than the actual measurement. This error is mainly caused by the assumption of a constant loss coefficient, which is difficult to modify in the SINDA/FLUINT input file based on the connection and flow conditions.

In the analyzed flow network shown in Fig. 1, gas stream flows into the manifold and three cross-ducts distribute the flow stream into the distribution manifold. Two manifolds are located at each end of the channels and connected by the cross-ducts. The cross-ducts correspond to channels C4, C11, and C18. From Fig. 4, the results of the LDV measurement show peaks in those three channels. Channel C4 is closest to the inlet and outlet side and has highest flow rate. The flow rate trend decreases away from the inlet and outlet side, which indicates flow favoring the shortest short path.

The design of the two-manifold connected by cross-ducts to distribute inlet or exit gas provides a way to adjust the peak flow position and also the flow distribution pattern. For achieving an optimum flow distribution, the flow network design is essential. With the aid of the flow distribution analysis through computation, the selection of the manifold size and network configuration for realizing a desired flow distribution become easy. In a flow network design, better flow uniformity may be achieved if the ratio of the pressure drop across the channels to the pressure drop in the plenum and other connecting ducts is maximized, without significant increases in the overall pressure drop. One design approach leading to a uniform flow distribution is to minimize the pressure drop in the plenum without significantly increasing the pressure drop in the channels.

4. Conclusions

The methodology used in the GT code for flow network analysis has been presented. The code includes transitional losses, based on the loss coefficients' data in Idelchik's flow handbook. The code can be used to describe the flow distribution through a complex network. The code provides added flexibility in modeling such networks, compared to SINDA/FLUINT, the commercially available flow network analysis code. An automatic loop identification and network equation generation code has been developed and shown to be consistent with the manually generated equations in the GT code.

Acknowledgements

The authors appreciate the effort of Mr. Dennis Sadowski and Mr. Joerg Stromberger in obtaining the experimental data. The first author also thanks Georgia Institute of Technology in providing research assistant position.

References

[1] Z. Ma, S.M. Jeter, Abdel-Khalik, Said, Modeling of Transport Processes Within a Molten Carbonate Fuel Cell Stack, ASME International Mechanical Engineering Congress and Exposition, New York, 2001.
[2] H. Hirata, M. Hori, Gas-flow uniformity and cell performance in a molten carbonate fuel cell stack, J. Power Sources 63 (1996) 115–120.
[3] D.L. Sadowski, et al., Investigation of 100 cm^2 Test Hardware Hydraulic Characteristics Via Theoretical, Experimental, and Numerical Tools, Final Report, Georgia Institute of Technology, Atlanta, Georgia, 1997.
[4] I.E. Idelchik, Handbook of Hydraulic Resistance, 2nd Edition, Hemisphere Publishing Corporation, New York, 1986.
[5] Iri, Masao, Network Flow, Transportation and Scheduling, Theory and Algorithms, Academic Press, New York, 1969.
[6] Cullimore and Ring Technologies Inc., SINDA/FLUINT, System Improved Numerical Differential Analyzer and Fluid Integrator, User's Manual, Littleton, Colorado, 1996.
[7] D.A. Savic, G.A. Walters, Integration of a model for hydraulic analysis of water distribution networks with an evolution program for pressure regulation, Microcomput. Civil Eng. 11 (1996) 87–97.